Redox Biology 50 (2022) 102255

Contents lists available at ScienceDirect

Redox Biology

journal homepage: www.elsevier.com/locate/redox

Selenoprotein K protects skeletal muscle from damage and is required for satellite cells-mediated myogenic differentiation☆

Shengchen Wang [a], Xia Zhao [a], Qingqing Liu [a], Yue Wang [a], Shu Li [a,**], Shiwen Xu [a,b,*]

[a] College of Veterinary Medicine, Northeast Agricultural University, Harbin, 150030, PR China
[b] Key Laboratory of the Provincial Education Department of Heilongjiang for Common Animal Disease Prevention and Treatment, College of Veterinary Medicine, Northeast Agricultural University, Harbin, 150030, PR China

ARTICLE INFO

Keywords:
Selenoprotein K
Skeletal muscle
Satellite cells
Myogenesis
Endoplasmic reticulum stress
Oxidative stress

ABSTRACT

The regeneration of adult skeletal muscle after injury is primarily initiated by satellite cells (SCs), but the regulatory mechanisms of cells committed to myogenic differentiation remain poorly explored. Small molecular selenoprotein K (SelK) plays crucial roles in the modulation of endoplasmic reticulum (ER) stress and against oxidative stress. Here, we first showed that SelK expression is activated in myogenic cells during differentiation both in vivo and in vitro. Meanwhile, loss of SelK delayed skeletal muscle regeneration, inhibited the development of myoblasts into myotubes, and was accompanied by reduced expression of myogenic regulatory factors (MRFs). Moreover, ER stress, intracellular reactive oxygen species (ROS), autophagy and apoptosis under myogenesis induction were more severe in SelK-deficient mice and cells than in the corresponding control groups. Supplementation with specific inhibitors to alleviate excessive ER stress or oxidative stress partly rescued the differentiation potential and formation of myotubes. Notably, we demonstrated that Self-mediated regulation of cellular redox status was primarily derived from its subsequent effects on ER stress. Together, our results suggest that SelK protects skeletal muscle from damage and is a crucial regulator of myogenesis.

1. Introduction

In adult mammals, skeletal muscle represents the most massive tissue in the body, contributing to 40–50% of the total body weight [1]. Following injury, skeletal muscle displays a powerful regenerative capacity that is attributed to the ordered regulation of a cascade of events initiated by satellite cells (SCs) [2,3]. To rehabilitate damaged areas of muscle fibers, mononuclear SCs are rapidly activated from quiescence to undergo proliferation. Subsequently, except for a small part of activated SCs returning to a quiescent state to replenish the stem pool, most SCs undergo myogenic differentiation and finally fuse into multinucleated myotubes or nascent myofibers [4–6]. This complex multistep process primarily relies on the specific expression of multiple myogenic regulatory factors (MRFs), such as Pax7 and the myogenic differentiation marker (MyoD) family, which determines the development and integrity of skeletal muscle regeneration [7]. Accumulating evidences have suggested that both deferred and premature differentiation can disturb the homeostasis of myogenesis and impair the performance of muscle remodelling [8,9].

Due to high metabolic activity after activation, SCs need to be exposed to an oxidative environment dominated by pro-oxidant signalling [10]. Some intracellular processes necessary for the myogenic differentiation of SCs, such as autophagy and apoptosis, are strongly related to oxidative stress [11,12]. However, the role of reactive oxygen species (ROS) generated in the matrix on the final maturation of skeletal muscle cells is complex and bifacial. The delicate balance between oxidative stress and antioxidant enzyme (e.g., SOD1, SOD2 and CAT) activities maintains muscle homeostasis [13]. ROS production beyond a threshold level can impair SCs differentiation and skeletal muscle regeneration. For instance, during amyotrophic lateral sclerosis or multiple cachexia syndrome, skeletal muscle degeneration is usually accompanied by excessive ROS production [14,15]. In addition, in cardiotoxin-induced muscle injury, artificial intervention in NOX4-mediated ROS production disrupted skeletal muscle regeneration and myoblast fusion [16]. Apart from oxidative stress, evidence has proven that the endoplasmic reticulum (ER) stress-induced unfolded

☆ All authors have read the manuscript and agreed to submit it in its current form for consideration and for publication in the Journal.

* Corresponding author. College of Veterinary Medicine, Northeast Agricultural University, Harbin, 150030, PR China.
** Corresponding author. College of Veterinary Medicine, Northeast Agricultural University, Harbin, 150030, PR China.
E-mail addresses: lishu@neau.edu.cn (S. Li), shiwenxu@neau.edu.cn (S. Xu).

https://doi.org/10.1016/j.redox.2022.102255
Received 29 November 2021; Received in revised form 23 January 2022; Accepted 28 January 2022
Available online 4 February 2022

protein response (UPR) signalling pathway also plays crucial roles in multifaceted regulation of myogenesis [17]. The ER is a network in the cytoplasm composed of branched ER tubules and flat capsules that is primarily responsible for coordinating the biosynthesis, folding and secretion of cellular proteins [18]. Disturbances in cellular homeostasis can result in an accumulation of unfolded/misfolded proteins in the ER lumen, with resultant ER stress [19]. To respond to ER stress, a signal transduction mechanism is activated, known as the unfolded protein response (UPR), which is driven by three ER transmembrane sensors (PERK, IRE1 and ATF6). These sensors reduce the accumulation of ER proteins by activating two mechanisms, the degradation of ER-associated resident proteins (ERAD) and the refolding of unfolded proteins [20,21]. The three arms of the UPR play a role in regulating the differentiation efficiency in different stages of the myogenesis process. It has been reported that prior to differentiation, ATF6 facilitates the apoptotic pruning process to eliminate differentiation-incompetent myoblasts [22]. During the early differentiation phase, the PERK/eIF2α/CHOP axis can be transiently activated, inhibiting the overexpression of MyoD and preventing premature differentiation [23]. IRE1 controls the fusion of myocytes into multinucleated myotubes [24].

Selenium is an essential trace element for organisms that is incorporated into selenoproteins in the form of selenocysteine to play important roles in many biological processes [25]. Patients with selenium deficiency often develop skeletal muscle disorders, such as muscle pain, proximal weakness and fatigue, emphasizing the potential functions of selenoproteins in regulating muscle homeostasis [26]. Selenoprotein K (SelK) is a small molecular selenoprotein (~12 kDa) located in the ER membrane that is closely related to immunity, cancer and development [27,28]. Although the functions of SelK include the maintenance of ERAD and antioxidants, and its expression has been detected in skeletal muscle [29–31], whether SelK participates in the reconstruction of skeletal muscle is entirely unknown. In the present study, SelK was found to be highly expressed in activated SCs in response to 1.2% $BaCl_2$ injury. Utilizing genetic mouse models, we demonstrated that SelK ablation inhibited SCs myogenic differentiation and delayed skeletal muscle repair. Mechanistically, SelK regulated ROS production by stabilizing ER stress to mediate autophagy and apoptosis.

2. Materials and methods

2.1. Animals

All procedures used in this experiment were approved by the Animal Care and Use Committee of Northeast Agricultural University (SRM-11). The generation of a SelK knockout (SelK KO) mouse model (C57BL/6) was achieved using CRISPR/Cas-mediated genome engineering. In brief, the mouse SelK gene (GenBank accession number: NM_019979.2; Ensembl: ENSMUSG00000042682) is located on mouse chromosome 14. We identified five exons from the SelK gene sequence, with the ATG start codon in exon 1 and the TAA stop codon in exon 5. Exon 1 to exon 5 were selected as target sites for insertion of two pairs of gDNA targeting vectors. Cas9 mRNA and gRNA generated by in vitro transcription were coinjected into fertilized eggs for KO mouse production.

2.2. Skeletal muscle injury and tissue section preparation

To induce skeletal muscle injury, 75 μl of $BaCl_2$ (1.2% in saline, Sigma-Aldrich) was injected into the tibial anterior (TA) muscle of 10-week-old mice. At 3, 5, and 7 d postinjury, the mice were sacrificed and then the TA muscles were harvested. Isolated muscle tissues were washed with normal saline and fixed in 4% paraformaldehyde for more than 48 h. After immersion fixation and dehydration embedding, 5 μm paraffin sections of the muscles were generated.

2.3. Histology and morphometric analysis

In order to evaluate the morphology and regeneration of TA muscle, paraffin sections of skeletal muscles at 0, 3, 5 and 7 d postinjury were subjected to hematoxylin and eosin (H&E) staining. ImageJ software was used to calculate the number of myofibers containing ≥2 centrally located nuclei and the cross-sectional area (CSA) in H&E-stained muscle sections.

2.4. Culturing of cell lines

For in vitro experiments, mouse C2C12 myoblasts were cultured as previously described [32]. Cultured cells were maintained in growth medium (DMEM high glucose (HyClone, Sigma-Aldrich) containing 10% FBS (Biological Industries (BI)) and 1% penicillin-streptomycin (Beyotime) on cell culture plates (Corning, Sigma-Aldrich) at 37 °C in a humidified atmosphere with 5% CO_2. To induce myogenic differentiation, the cell line at 80% confluency was changed from growth medium to differentiation medium (DMEM high glucose containing 2% horse serum (Beyotime) and 1% penicillin-streptomycin).

2.5. Transfections and processing

For SelK knockdown in vitro, C2C12 myoblasts were cultured in 6-well plates containing growth medium until the confluency reached 60–70%. Subsequently, cells were transfected with siRNAs using Lipofectamine RNAi MAX transfection reagent (Invitrogen) according to the method described by Chi et al. [33]. Cells transfected with stealth RNAi Negative Control (siNC) were used as controls. The target sequence used for silencing of mouse SelK (siSelK) was 5′-GAA GAG GCT ACG GGA GCT CC-3′, and siSelK and siNC were designed by RiboBio. After 12 h of transfection, the cells were washed once with PBS and incubated with differentiation medium to induce the formation of myotubes. N-acetyl cysteine (NAC) and sulforaphane (SF) are commonly used antioxidant regents, and 4-phenylbutyrate (4-PBA) and tauroursodeoxycholic acid (TUDCA) are potent inhibitors of ER stress. Considering the key role of changes in oxidative stress and ER stress levels in myogenic differentiation, we treated cells with NAC (1 mM) or SF (1 μm) to restrain ROS production and 4-PBA (1 mM) or TUDCA (200 μm) to restrain ER stress during differentiation phases (days 1–5).

2.6. Apoptosis analysis

We used TdT-mediated dUTP nick-end labeling (TUNEL) staining to assess apoptosis in TA muscles. Briefly, 5 μm paraffin-embedded sections were incubated in permeabilization solution and treated with an in situ apoptosis detection kit (Roche). Subsequently, 10 μg/mL 4,6-diamidino-2-phenylindole (DAPI) was used to localize the nuclei of cells and stain them to blue, and apoptotic cells were stained green by the TUNEL reaction mixture. Meanwhile, acridine orange/ethidium bromide (AO/EB) dual staining and flow cytometry were employed to analyse apoptosis. For AO/EB staining, cells cultured in growth or differentiation medium were rinsed with PBS and stained with AO/EB working solution (20 μL/mL) for 5 min. Then, the fluorescence signal was imaged under a fluorescence microscope. For flow cytometry, cells were labelled with propidine iodide (PI) and Annexin V according to the manufacturer's instructions (KENGEN Biotech). The methods for calculating the rate of apoptosis were provided by FlowJo software.

2.7. Detection of antioxidant function

To identify the effect of SelK on the levels of oxidative stress during skeletal muscle injury repair, commercial chemical test kits purchased from Jiancheng Bioengineering Institute were employed to determine the activities of superoxide dismutase (SOD), catalase (CAT) and total antioxidant capacity (T-AOC) and the contents of peroxidative

decomposition products (hydrogen peroxide (H_2O_2), malonic dialdehyde (MDA)). In brief, fresh TA muscle tissues at 3 d postinjury were homogenized in cold physiological saline solution and centrifuged at 3500 r for 15 min. Then, the obtained supernatants were used to measure changes in these oxidative stress markers according to the manufacturer's instructions.

2.8. Detection of intracellular ROS generation

We used a 2′,7′-dichlorodihydrofluorescein diacetate (DCFH-DA) kit provided by Jiancheng Bioengineering Institute to observe and analyse the production of intracellular ROS. After removing the medium, the cells were washed with PBS and treated with serum-free medium containing DCFH-DA (a sensitive probe that can be oxidized by intracellular ROS to the fluorescent 2,7-dichlorofuorescin (DCF)) for 30 min. Then, images of fluorescent ROS labelled with DCF were obtained using fluorescence microscopy, and ROS production was quantified by using a fluorescence microplate reader.

2.9. Immunohistochemistry and immunofluorescence

For immunohistochemistry, paraffin sections of TA muscles fixed in 4% PFA were permeabilized in 0.3% Triton X-100 for 20 min. After treatment with 3% H_2O_2 for 15 min and blocking in blocking buffer (Servicebio) for 2 h, samples were then incubated with primary antibodies (diluted in PBST) at 4 °C overnight. Subsequently, the sections were rinsed in TBST and incubated with biotin-conjugated secondary antibody at room temperature for 1 h. Finally, samples were stained with HRP-labelled streptavidin and the signal was developed with DAB (Servicebio). The primary antibodies used for immunohistochemistry were as follows: mouse anti-Pax7 (cat. No. sc-81648, Santa Cruz, 1:50), rabbit anti-SelK (cat. No. ab139949, Abcam, 1:50), and mouse anti-MyoG (cat. No. GB14118, Servicebio, 1:50).

For immunofluorescence and cell staining, after fixation in 4% PFA and permeabilization in 0.3% Triton X-100 for 20 min, the sample sections and cultured cells were blocked with blocking buffer (Servicebio) for 2 h at room temperature and incubated with primary antibodies at 4 °C overnight. Subsequently, the samples were washed with TBST and incubated Secondary antibody with fluorescent label. The primary antibodies used in immunofluorescence were as follows: rabbit anti-Ki67 (cat. No. GB13030-2, Servicebio, 1:200), mouse anti-Pax7 (cat. No. sc-81648, Santa Cruz, 1:50), rabbit anti-SelK (cat. No. ab139949, abcam, 1:50), mouse anti-MyoG (cat.no. GB14117, Servicebio, 1:200), mouse anti-MyoD (cat.no. GB14116, Servicebio, 1:200), mouse anti-MyHC (cat.no. sc-81648 1:50), rabbit anti-p62 (cat.no. GB11239-1, Servicebio, 1:200) and rabbit anti-LC3B (cat.no. A19665, ABclonal).

2.10. Analysis of cell number and the cell cycle

A Cell Counting Kit-8 assay (CCK-8) assay was used to complete the detection of cell number. In brief, after transfection, C2C12 myoblasts were cultured in 96-well plates for 24 h and 48 h, respectively. Then, 10 μL of CCK-8 reagent (Saint-Bio) was add into each well for 1 h, and the absorbance reads at 490 nm ($n = 6$) were identified by using an Infinite F50 microplate reader (Tecan). For the cell cycle, transfected C2C12 myoblasts in 6-well plates were fixed in 70% ethanol at −20 °C overnight. After washing twice with PBS and treating with a Cell Cycle Detection Kit (KeyGen BioTECH) at temperature for 1 h without light, the red fluorescence at an excitation wavelength of 488 nm was recorded by using flow cytometry (Becton Dickinson, FACSCalibur). The cell cycle was analysed by using ModFit LT (Verity Software House).

2.11. Quantitative real-time PCR (qRT–PCR)

Total RNA was obtained from TA muscles and treated cells with TRIzol reagent (Invitrogen, Thermo Fisher Scientific), and the concentration and purity of RNA were measured using a spectrophotometer at 260/280 nm. First-strand cDNA for qRT–PCR was generated using a commercial synthesis kit (Bioer Technology). The primers were designed using online primer design software (Sangon Biotech) and are shown in Table S1. The quantification of mRNA expression was performed using a BioRT Real Time RT–PCR Kit (Bioer Technology) in a LineGene 9600 Plus (Bioer Technology). GAPDH was used as a housekeeping gene to complete data normalization according to the 2-ΔΔCt method.

2.12. Western blotting

Western blotting was performed as previously described [34]. In brief, skeletal muscle and treated cells were lysed in ice-cold RIPA buffer with PMSF protease inhibitor (Beyotime). The supernatant was obtained by centrifugation, and the concentration of protein was determined by a BCA assay kit (Beyotime). Equal amounts of proteins from different groups were loaded and separated on 6–15% SDS–PAGE gels, transferred onto nitrocellulose membranes (Pall Corporation) and blocked for 2 h at 37 °C with 5% milk-TBST. Membranes were incubated either overnight at 4 °C with primary antibodies against: SelK (Abcam, 1: 500), MyoD (Abclonal, 1:1000), MyoG (Abclonal, 1:1000), MyHC (Abclonal, 1:1000), GRP78 (Abclonal, 1:1000), ATF6 (Abclonal, 1:1000), phospho-IRE1 (p-IRE1, Abclonal, 1:500), phospho-PERK (p-PERK, Abclonal, 1:500), phospho-eIF-2α (p-eIF-2α, Abclonal, 1:1000), CHOP (Abclonal, 1:1000), LC3B (Abclonal, 1:1000), p62 (Abclonal, 1:1000), cleaved Caspase3 (cle-Cas3, Abclonal, 1:1000), Bcl2, Bax (My lab, 1:400) and GAPDH (Servicebio, 1:1000). Then, the membranes were washed with TBST three times and incubated with HRP-conjugated secondary antibodies (ImnunoWay, 1: 8000) at temperature for 1 h. The bands were visualized by using an ECL kit (Kangweishiji Biotechnology) and an Azure imaging Biosystem C300.

2.13. Statistical analyses

All data presented in the present study were collected from at least three biological replicates. The results are expressed as the means ± standard error of the mean (SEM). Data were analysed by one-way ANOVA of variance or unpaired *t*-test using GraphPad Prism software 7, and a p-value < 0.05 was considered statistically significant: $^*p < 0.05$, $^{**}p < 0.01$ and $^{***}p < 0.001$. The software showed that data had a normal distribution.

3. Results

3.1. SelK is upregulated in differentiated myogenic cells

To examine the role of SelK during skeletal muscle regeneration, we analysed the expression of SelK in SCs by immunostaining of myofibers isolated from TA muscles injured with $BaCl_2$ injection. However, in Pax7-quiescent SCs, no obvious SelK protein expression was observed (Fig. 1A and Fig. S1A), but we observed that SelK was significantly expressed in Pax7-positive ($Pax7^+$) SCs and MyoG-activated ($MyoG^+$) myogenic cells (Fig. 1B, C and Figs. S1B and C). Meanwhile, SelK levels in the TA muscles of $BaCl_2$-injured mice were detected, and the expression levels of SelK were significantly higher in the injured than in the control TA muscles (treated with mock saline) at 5 d postinjury (Fig. 1D). Furthermore, to analyse SelK expression in vitro, C2C12 myoblast cells were incubated and allowed to differentiate into myotubes. As the differentiation degree of C2C12 myoblasts increased, expression of SelK was gradually promoted (Fig. 1E–H). Taken together, these data indicate that the transcriptional levels of SelK are remarkably elevated in differentiated myogenic cells.

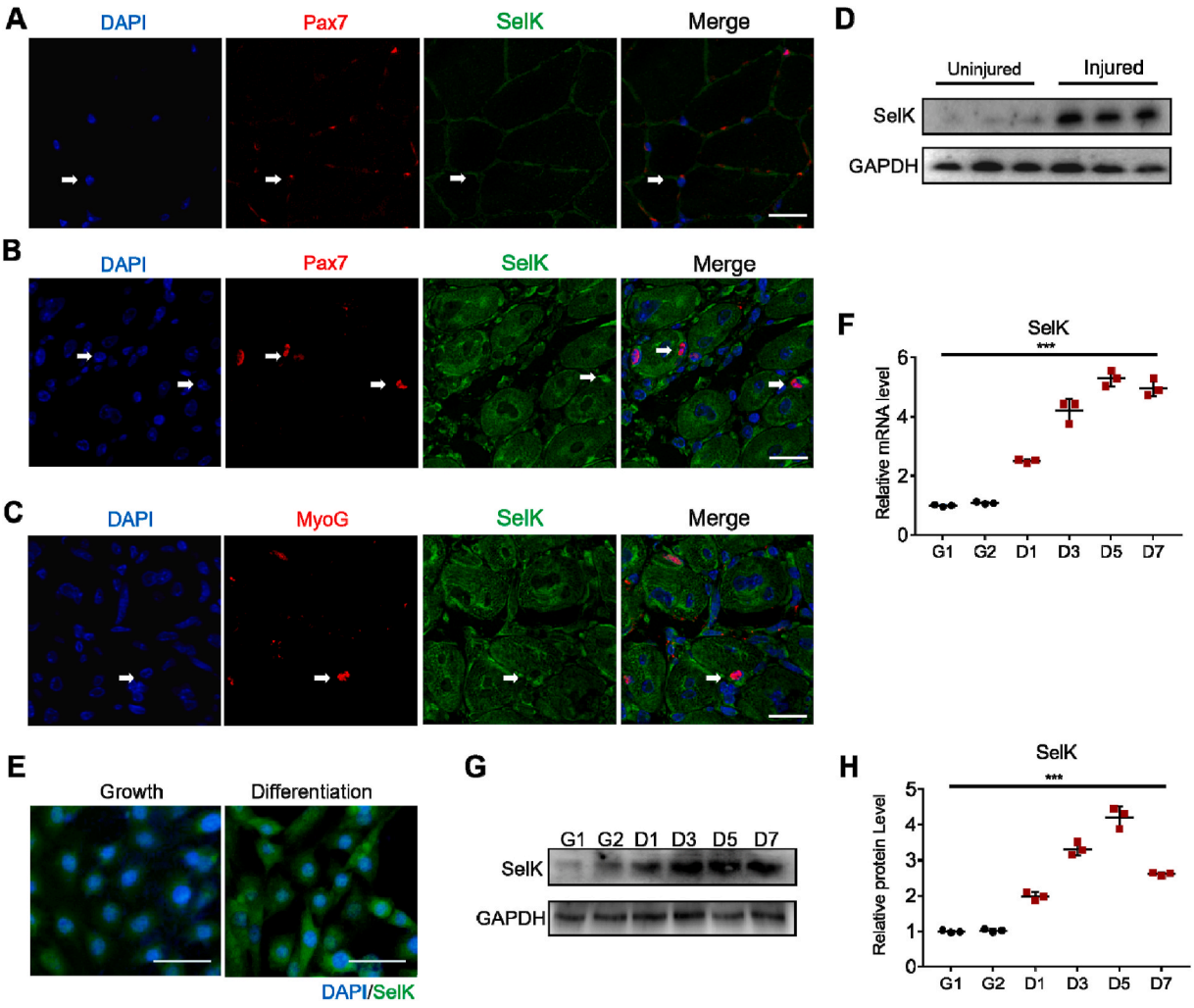

Fig. 1. SelK is upregulated in during SCs differentiation and C2C12 myoblast differentiation. (A) Immunofluorescence staining of Pax7 (red) and SelK (green) in TA muscle of wild-type mice without 1.2% $BaCl_2$ injection. Scale bar = 50 μm. **(B)** Immunofluorescence staining of Pax7 (red) and SelK (green) in TA muscle of wild-type mice at 5 d postinjury. Scale bar = 50 μm. **(C)** Immunofluorescence staining of MyoG (red) and SelK (green) in TA muscles of wild-type mice at 5 d postinjury. Scale bar = 50 μm. **(D)** Western blot analysis of SelK protein levels in uninjured and 5 d-injured TA muscle. N = 3 mice in each group for A-D. **(E)** Immunofluorescence staining of SelK in C2C12 myoblasts cultured in growth medium for 1 d or in differentiation medium for 2 d. Scale bar = 50 μm. **(F)** qRT-PCR analysis of SelK mRNA levels in C2C12 myoblasts cultured in growth medium for 1 or 2 d (G1 or G2) or in differentiation medium for 1, 3, 5 or 7 d (D1, D3, D5 or D7). **(G)** and **(H)** Western blotting analysis of SelK protein levels in C2C12 myoblasts cultured in growth or differentiation medium for 1 or 2 d (G1 or G2) or in differentiation medium for 1, 3, 5 or 7 d (D1, D3, D5 or D7). N = 3 in each group for E-H. The results are presented as means ± S.D. ***$p < 0.001$, values significantly different from the corresponding control by unpaired *t*-test. (For interpretation of the references to colour in this figure legend, the reader is referred to the Web version of this article.)

3.2. SelK ablation causes inefficient regeneration of adult skeletal muscle

Although we found that expression of SelK was upregulated during the process of myogenic differentiation, we still needed to determine whether it plays a positive or negative function in myogenic differentiation. Thus, we generated SelK knockout (SelK KO) mice using CRISPR/Cas-mediated genome engineering (Fig. 2A and B). Under normal conditions, the SelK KO mice displayed similar weight and health status as wild-type mice, and ablation of SelK did not affect the ratio of TA muscle weight to whole body weight (Fig. 2C and D). To investigate the role of SelK in skeletal muscle regeneration, we injected $BaCl_2$ into the TA muscles of mice in the control and SelK KO groups. Immunostaining revealed that SelK was successfully deleted in $Pax7^+$ and $MyoG^+$ cells of SelK KO mice compared to the control group at 5 d postinjury (Fig. 2E). Meanwhile, the effect of SelK deletion on regeneration after skeletal muscle injury was examined by using H&E staining. When uninjured, no difference was observed in the cross-sectional size of muscle fibers between wild-type mice and SelK KO mice (Fig. 2F). Intriguingly, compared to the normal muscle regeneration process in control mice at 3, 5 and 7 d postinjury, SelK KO mice displayed delayed muscle recovery (Fig. 2F). The numbers of regenerating myofibers containing two or more central nuclei were also notably decreased in SelK KO mice (Fig. 2G). Moreover, the average cross-sectional area (CSA) of myofibers in SelK KO mice was significantly decreased by 25% compared to that in control mice at 5 days of injury (Fig. 2H). In agreement with this, further analysis of the average areas of myofibers with centralized nuclei showed that most of the muscle fiber areas in SelK KO mice were less than 400 μm^2, while in contrast, the muscle fiber areas in control mice were primarily distributed in the range of 400 and 600 μm^2 (Fig. 2I). The impaired regenerative capability of TA muscles in SelK KO mice was also evidenced by the reduced size of fibers positive for MyHC ($MyHC^+$) (Fig. 2J and K). Overall, these findings demonstrate that SelK exerts a positive regulatory effect on muscle regeneration and that its inactivation impairs SCs function.

3.3. SelK ablation inhibits the myogenic differentiation in vivo

When quiescent SCs are activated by stress, they acquire MyoD

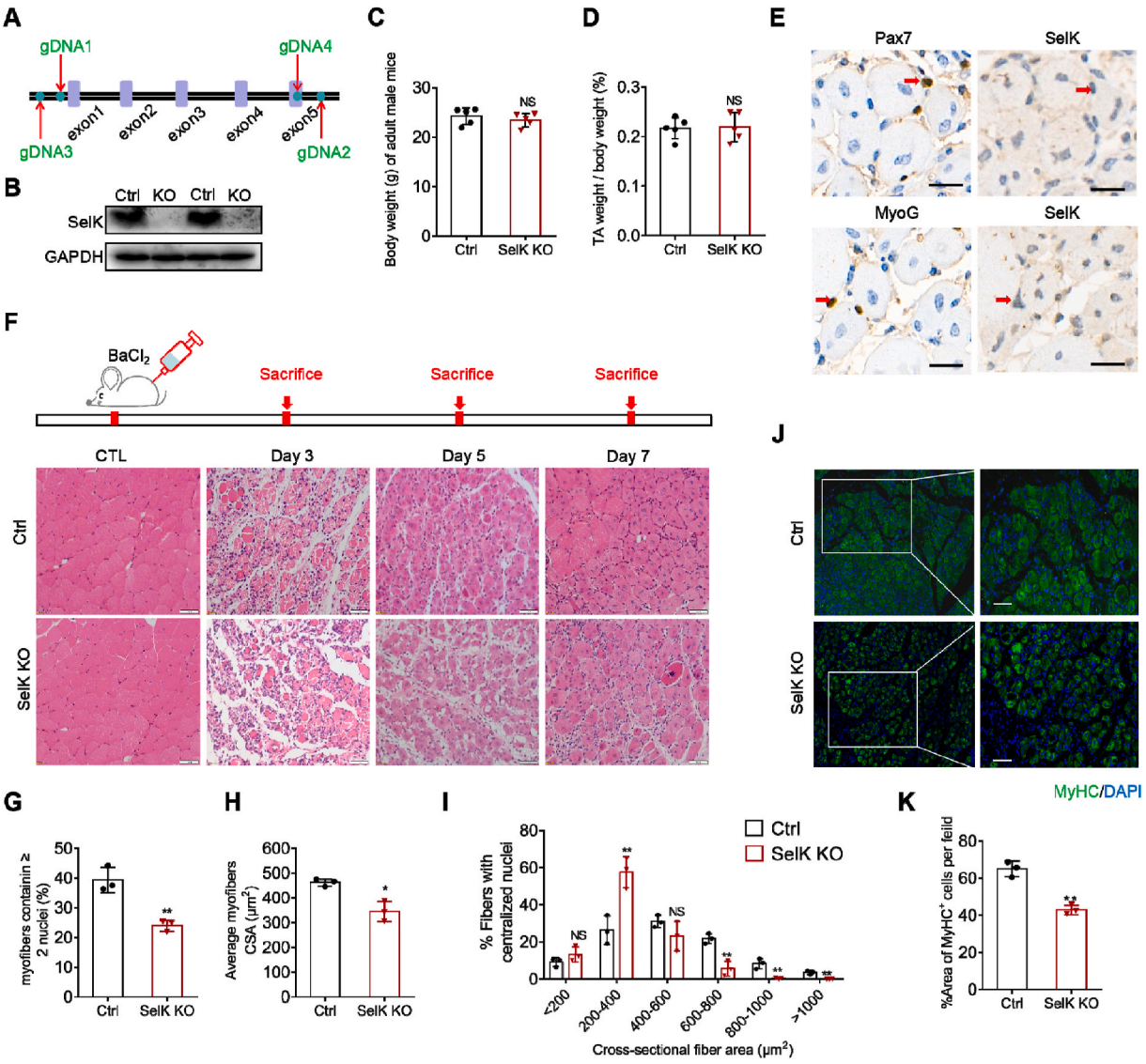

Fig. 2. Ablation of SelK impairs skeletal muscle regeneration. (A) A schematic illustration of the knockout of SelK using CRISPR/Cas-mediated genome engineering. **(B)** Western blotting analysis of SelK protein levels in the TA muscle of wild-type (Ctrl) mice and SelK KO mice at 5 d postinjury (N = 3). **(C)** Average overall body weight of adult wild-type mice and SelK KO mice (N = 5). **(D)** Relative uninjured TA muscle wet weight of adult wild-type and SelK KO mice (N = 5). **(E)** Immunohistochemistry analysis of SCs markers (Pax7 and MyoG) and SelK in the TA muscle of SelK KO mice at 5 d postinjury (N = 3). Scale bar = 50 μm. **(F)** H&E staining of TA muscle in adult Ctrl and SelK KO mice at 0, 3, 5 and 7 d postinjury (N = 3). Scale bar = 50 μm. **(G)** Rate of myofibers containing two or more centrally located nuclei per field and **(H)** the average cross-sectional area (CSA) of myofibers calculated from TA muscle of Ctrl and SelK KO mice at 5 d postinjury (N = 3). **(I)** Distribution of regenerative myofiber CSAs of Ctrl and SelK KO mice at 5 d postinjury (N = 3). **(J)** Immunofluorescence staining of MyHC (green) in TA muscles of Ctrl and SelK KO mice at 5 d postinjury (N = 3) and **(K)** the percentage of MyHC-positive ($MyHC^+$) fibers in TA muscle of Ctrl and SelK KO mice at 5 d postinjury. Nuclei were labelled using DAPI staining. Scale bar = 50 μm. The results are presented as means ± S.D. *$p < 0.05$, **$p < 0.005$, values significantly different from the corresponding control by unpaired *t*-test. (For interpretation of the references to colour in this figure legend, the reader is referred to the Web version of this article.)

expression ($Pax7^+MyoD^+$), and are then classified as proliferative muscle progenitor cells. Subsequently, most progenitor cells exit the cell cycle and lose Pax7 ($Pax7^-MyoD^+$) to enter myogenic differentiation. Finally, they gain MyoG, and initially coexpress with MyoD followed by independent expression of MyoG [35,36]. The impact of SelK ablation on skeletal muscle regeneration encouraged us to investigate the importance of SelK in the process of SCs differentiation. Therefore, to explore whether the differentiating potential of SCs is modulated by SelK expression in vivo, TA muscles from both genotypes were stained for Pax7 and MyoD at 3 d post-$BaCl_2$ injection. As shown in Fig. 3A and B, SelK inactivation markedly decreased the percentage of cell populations belonging to the differentiated $Pax7^-MyoD^+$ population but increased $Pax7^+MyoD^-$ quiescent cell numbers. Meanwhile, at 5 d postinjury, compared to wild-type mice, the share of $MyoD^-MyoG^+$ and $MyoD^+MyoG^+$ was significantly lower in SelK KO muscles, while that of $MyoD^+MyoG^-$ SCs was higher (Fig. 3C and D). To confirm this observation, we quantified the expression of MRFs in TA muscles at the gene and protein levels. Consistently, mRNA expression of the primary MRFs (MyoD1, MyoG, MyH1, MyH2 and MyH3) and protein expression of MyoD, MyoG and MyHC were significantly reduced in SelK KO mice (Fig. 3E–G). Thus, our results suggest that loss of SelK delays the myogenic differentiation of SCs in vivo.

3.4. Silencing of SelK inhibits myogenic differentiation in vitro

To further elucidate the role of SelK in regulating the balance of myogenic differentiation, we silenced SelK in C2C12 myoblasts using siRNA transfection (siSelK) and induced the formation of myotubes. As

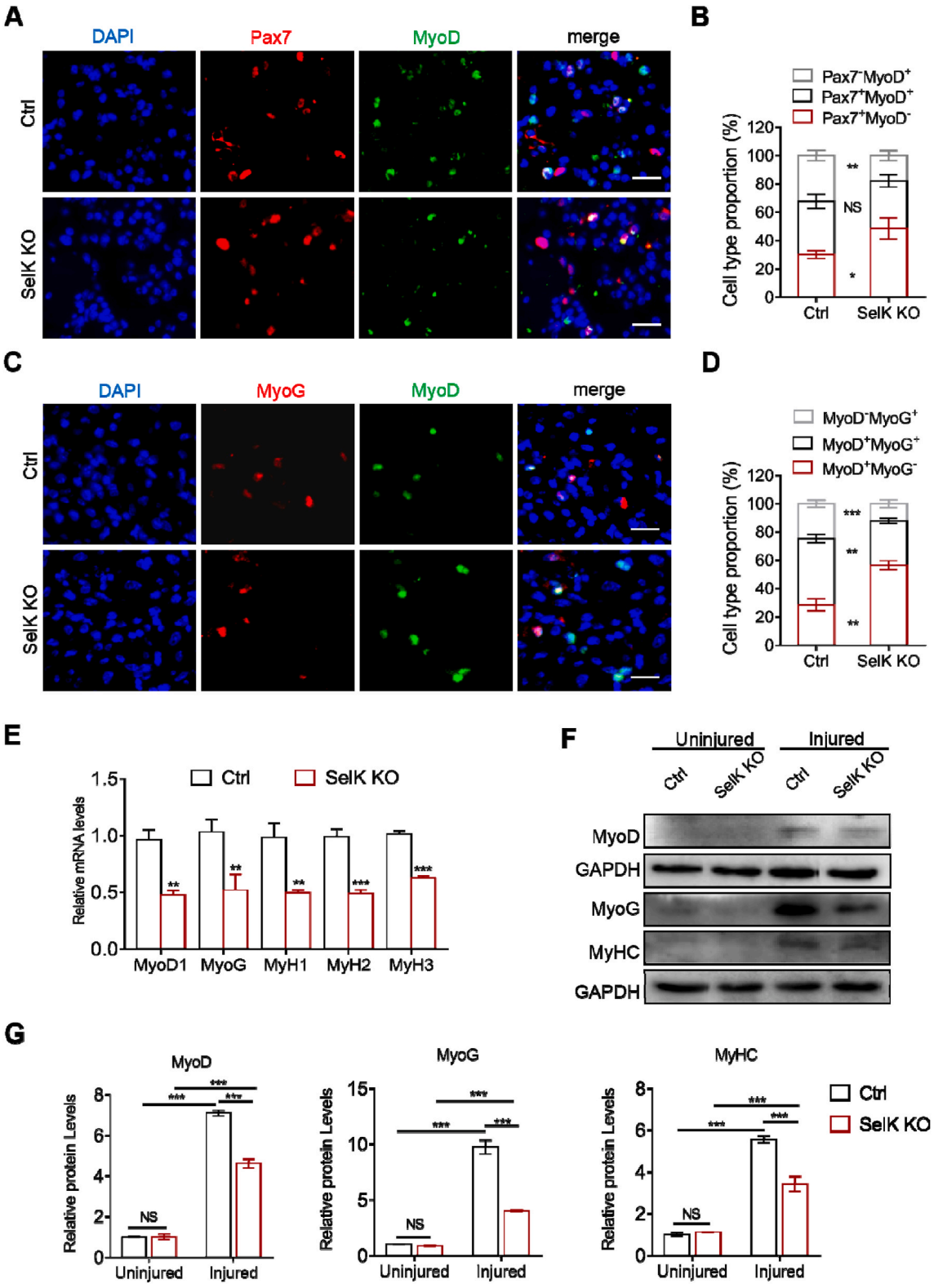

Fig. 3. Inactivation of SelK inhibits the myogenic differentiation progression of SCs. (A) Immunofluorescence staining of MyoD (green) and Pax7 (red) in TA muscle of Ctrl and SelK KO mice at 3 d postinjury (N = 3). Nuclei were labelled using DAPI staining. Scale bar = 20 μm. **(B)** Quantification of the percentages of $Pax7^{+}MyoD^{-}$, $Pax7^{+}MyoD^{+}$ and $Pax7^{-}MyoD^{+}$ cell populations in Ctrl and SelK KO TA muscles at 3 d postinjury. **(C)** Immunofluorescence staining of MyoD (green) and MyoG (red) in TA muscle of Ctrl and SelK KO mice at 5 d postinjury (N = 3). Nuclei were labelled using DAPI staining. Scale bar = 20 μm. **(D)** Quantification of the percentages of $MyoD^{+}MyoG^{-}$, $MyoD^{+}MyoG^{+}$ and $MyoD^{-}MyoG^{+}$ cell populations in Ctrl and SelK KO TA muscles at 5 d postinjury. **(E)** qRT-PCR analysis of myogenic transcription factors (MyoD1, MyoG, MyH1, MyH2 and MyH3) mRNA levels in TA muscle of Ctrl and SelK KO mice at 5 d postinjury (N = 3). **(F)** and **(G)** Western blotting analysis of MyoD, MyoG and MyHC protein levels in uninjured and 5 d-postinjured TA muscle of Ctrl and SelK KO mice (N = 3). The results are presented as means ± S.D. *$p < 0.05$, **$p < 0.005$, ***$p < 0.001$, values significantly different from the corresponding control by unpaired *t*-test. (For interpretation of the references to colour in this figure legend, the reader is referred to the Web version of this article.)

shown in Fig. 4A–C, we found that throughout the differentiation process (days 1 to day 5), expression of SelK was still lower than that of the control group (day 0), indicating satisfactory knockdown efficiency. As expected, consistent with the in vivo results, siSelK transfection diminished C2C12 myoblast differentiation (Fig. S2). This finding was accompanied by a decrease in the myotube formation of approximately 80% after inducing differentiation (Fig. 4D and E). Meanwhile, we also found that compared to controls, the numbers of MyoG$^+$ C2C12 myoblasts were considerably reduced in the siSelK group (Fig. 4F and G). In addition, immunoblotting analysis of MyoD, MyoG and MyHC further demonstrated the inhibitory effect of siSelK on the differentiation of C2C12 myoblasts (Fig. 4H and I). These results suggest that genetic silencing of SelK inhibits myogenic differentiation in vitro.

3.5. Deletion of SelK has no effect on the proliferation of SCs

In addition, we also analysed the proliferative potential of SelK-silenced SCs during muscle regeneration. Immunostaining of Ki67, a marker protein presents in nuclei of proliferating cells was performed in the TA muscles of control and SelK KO mice at 3 days after $BaCl_2$ injury. The results demonstrated that the frequency and number of Ki67-positive cells (Ki67$^+$) were not significantly changed compared to control mice (Fig. 5A and B). Meanwhile, coimmunostaining for Pax7 and Ki67 on transverse sections was also conducted to determine the proliferation state of SCs, and the results showed that the percentage of Pax7$^+$Ki67$^+$ proliferating SCs in SelK KO muscles was equivalent to the double-positive rate in the control muscles (Fig. 5C and D). This finding also coincided with the fact that there was no significant difference between the percentage of cell populations belonging to proliferative Pax7$^+$MyoD$^+$ in TA muscles in the two genotypes (Fig. 4A and B). Furthermore, C2C12 myoblast cells transfected with siRNA specifically designed for SelK revealed that during the proliferation phase (1 and 2 days), SelK knockdown did not change the cell viability or cycle phase compared to cells transfected with negative control siRNA (siNC)

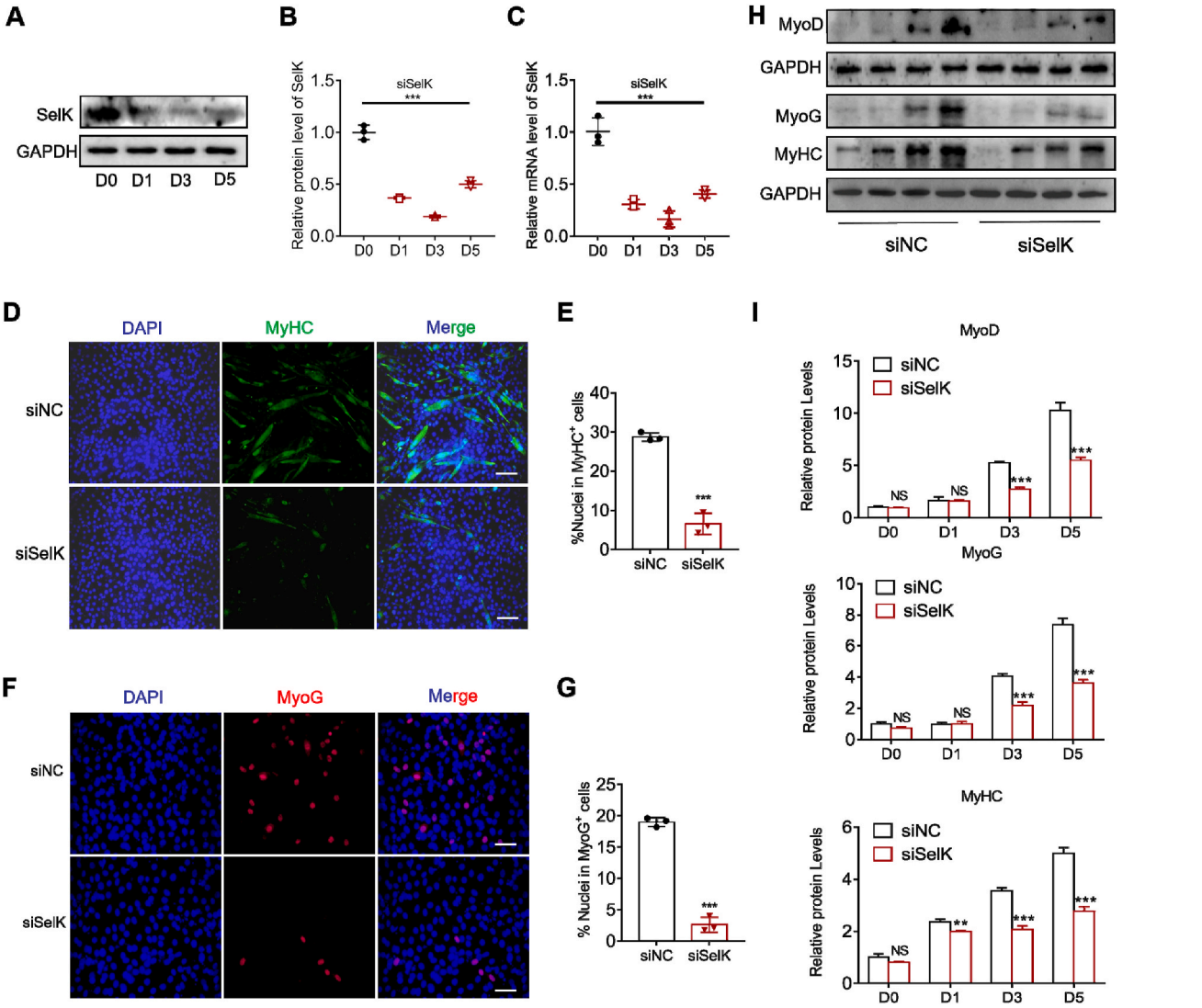

Fig. 4. The differentiation ability of C2C12 myoblast cells is reduced by SelK silencing. (A) and **(B)** Western blotting analysis of SelK protein levels in siSelK-transfected C2C12 myoblast cells cultured in differentiation medium for 1, 3 and 5 d (N = 3). **(C)** qRT-PCR analysis of SelK mRNA levels in siSelK-transfected C2C12 myoblast cells cultured in differentiation medium for 0, 1, 3 and 5 d (N = 3). **(D)** Immunofluorescence staining of MyHC in control siRNA (siNC) and SelK siRNA (siSelK) C2C12 myoblast cells cultured in differentiation medium for 5 d (N = 3). Scale bar = 100 μm. **(E)** Quantitative analysis of the percentage of MyHC$^+$ C2C12 myoblast cells. **(F)** Immunofluorescence staining of MyoG in siNC and siSelK C2C12 myoblast cells cultured in differentiation medium for 5 d (N = 3). Scale bar = 50 μm. **(G)** Quantitative analysis of the percentage of MyoG$^+$ C2C12 myoblast cells. **(H)** and **(I)** Western blotting analysis of MyoD, MyoG and MyHC protein levels in siNC and siSelK C2C12 myoblast cells cultured in differentiation medium for 0, 1, 3 and 5 d (N = 3). The results are presented as means ± S.D. **p < 0.005, ***p < 0.001, values significantly different from the corresponding control by unpaired *t*-test.

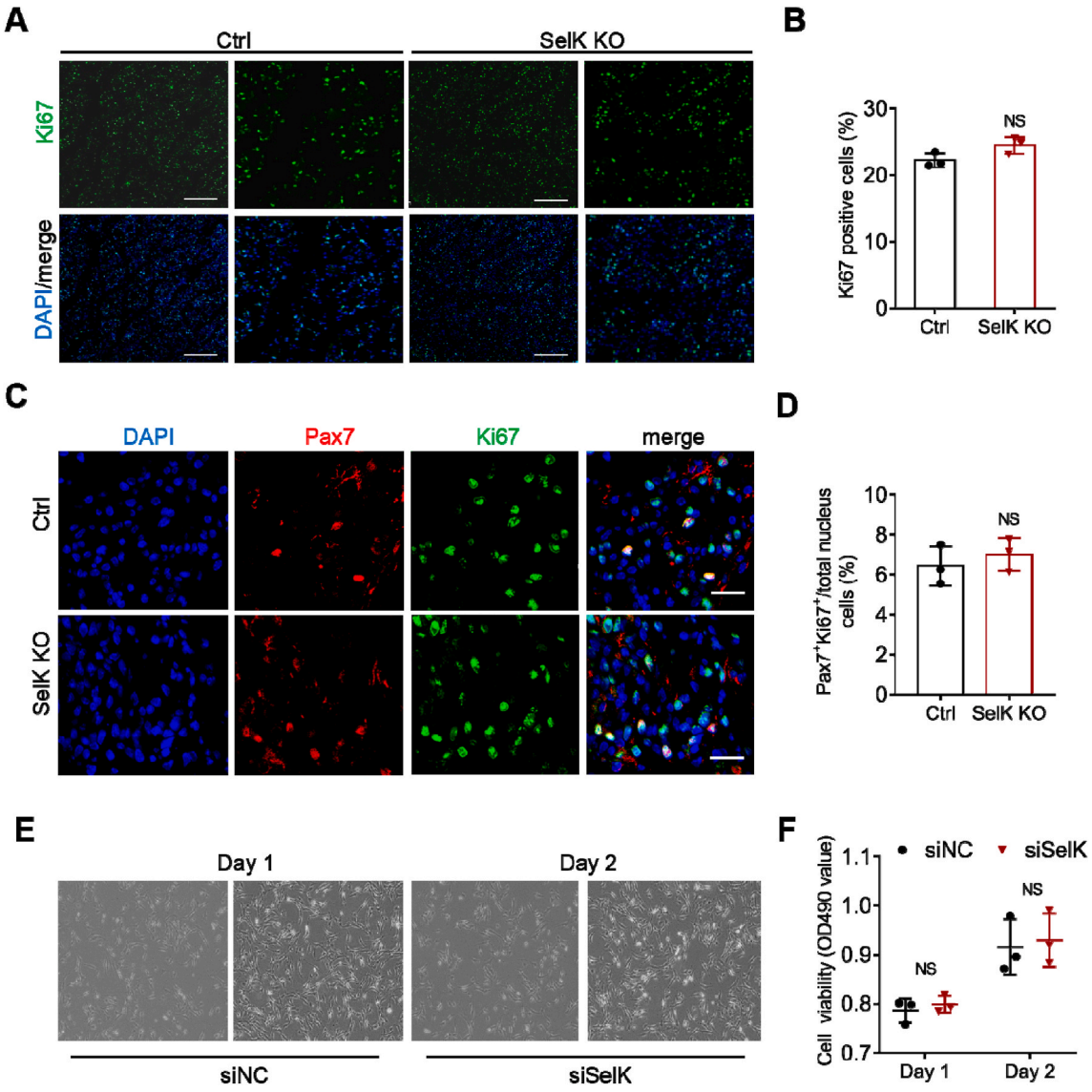

Fig. 5. The proliferation ability of SCs or C2C12 myoblast cells is not impaired in SelK KO mice. (A) Immunofluorescence staining of Ki67 (green) in TA muscles of Ctrl and SelK KO mice at 3 d postinjury (N = 3) and **(B)** the percentage of Ki67-positive ($Ki67^+$) cells per captured field. Nuclei were labelled using DAPI staining. Scale bar = 200 μm. **(C)** Immunofluorescence staining of Ki67 (green) and Pax7 (red) in TA muscle of Ctrl and SelK KO mice at 3 d postinjury (N = 3). Nuclei were labelled using DAPI staining. Scale bar = 20 μm. **(D)** Quantification of the percentage of $Pax7^+Ki67^+$ cells per captured field. **(E)** Bright field microscopy images of siNC and siSelK C2C12 myoblast cells cultured in growth medium for 1 or 2 d (N = 3). **(F)** CCK-8 assay of the viability of siNC and siSelK C2C12 myoblast cells cultured in growth medium for 1 or 2 d (N = 3). The results are presented as means ± S.D and analysed by unpaired *t*-test. (For interpretation of the references to colour in this figure legend, the reader is referred to the Web version of this article.)

(Fig. 5E, F and Fig. S3), highlighting the possibility that deficiency of SelK does not impair skeletal muscle regeneration by affecting the proliferation potential of SCs.

3.6. *Targeted deletion of SelK exacerbates apoptosis and autophagy in myogenic cells during myogenesis*

Previous studies have found that both apoptosis and autophagy regulate the activation of SCs and skeletal muscle regeneration [37]. However, dysregulated activation of these two processes can hinder myogenic differentiation [24]. Thus, we next examined the effect of SelK ablation on apoptosis and autophagy during skeletal muscle regeneration. As shown in Fig. 6A, $TUNEL^+$ cells were not found in sections from uninjured controls or SelK KO TA muscles, while 5 d postinjured TA muscles in SelK KO mice exhibited more $TUNEL^+$ cells than in corresponding injured TA muscle of control mice (Fig. 6A and B). Meanwhile, AO/EB staining was used to assess apoptosis in C2C12 myoblasts modulated by SelK during myogenic differentiation. The result showed that although the apoptotic rate of myoblasts in the control group varied with the differentiation phase, siSelK significantly increased the apoptotic rate in the corresponding period (Fig. 6C and D). Next, immunofluorescence staining revealed increased expression of the autophagy biomarkers LC3B and p62 in injured muscles, indicating the occurrence of autophagy in response to muscle damage. Notably, we clearly observed that compared to control mice, the relative fluorescence intensities of LC3B and p62 were significantly increased and decreased, respectively, in TA muscle sections of SelK KO mice (Fig. 6E and F). Furthermore, quantitative analysis of apoptosis- and autophagy-related markers (cle-Cas3, Bax, Bcl2, LC3 I/II and p62) using immunoblotting showed consistent results. SelK KO muscle or siSelK C2C12 myoblasts displayed increased cleaved Cas3, Bax:Bcl2 ratio, LC3 II:LC3 I ratio and decreased p62 compared to the corresponding control group (Fig. 6G, H and Fig. S4). Together, these results indicated that SelK ablation aggravates apoptosis and autophagy in myogenic cells

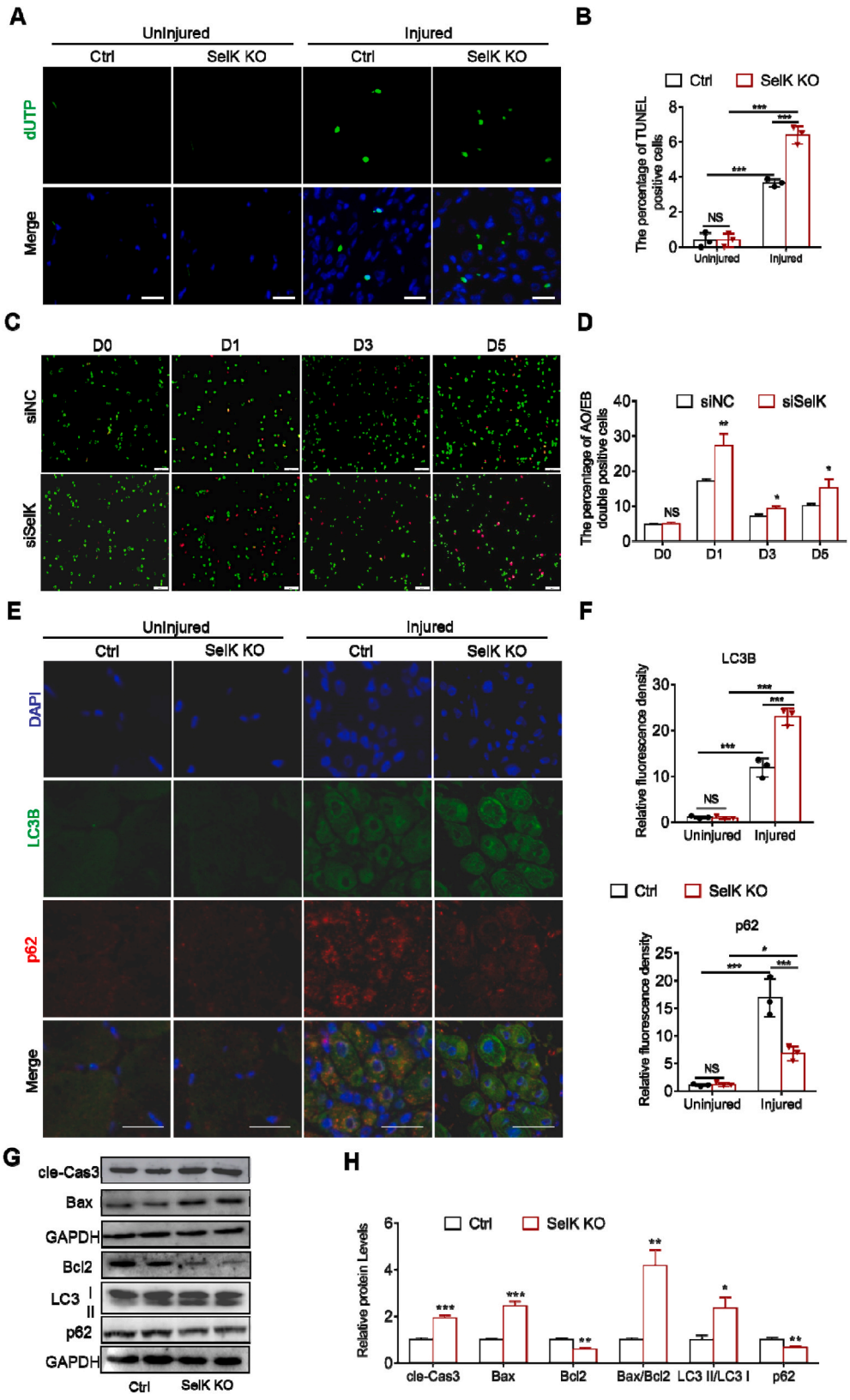

Fig. 6. Ablation of SelK aggravates apoptosis and autophagy in SCs and C2C12 myoblast cells during myogenic differentiation. (A) TUNEL staining of uninjured and 5 d 1.2% $BaCl_2$-postinjured TA muscles of Ctrl and SelK KO mice and **(B)** the quantification of TUNEL-positive cells (N = 3). Nucleus were labelled through DAPI staining. Scale bar: 50 μm. **(C)** AO/EB staining of siNC and siSelK C2C12 myoblast cells cultured in differentiation medium for 0, 1, 3 and 5 d and **(D)** the quantification of apoptotic cells (N = 3). Scale bar: 100 μm. **(E)** Immunofluorescence staining of LC3B (green) and p62 (red) in uninjured and 5 d-postinjured TA muscle of Ctrl and SelK KO mice (N = 3) and **(F)** the relative fluorescence density of LC3B and p62 per captured field. Nucleus were labelled through DAPI staining. Scale bar = 20 μm. **(G)** and **(H)** Western blotting analysis of apoptosis-related genes (Bax, Bcl2 and cle-Cas3) and autophagy-related genes (LC3I/II and p62) protein levels in TA muscle of Ctrl and SelK KO mice at 5 d postinjury (N = 3). The results are presented as means ± S.D. Results are presented as means ± S.D. *p < 0.05, **p < 0.005, ***p < 0.001, values significantly different from the corresponding control by unpaired *t*-test. (For interpretation of the references to colour in this figure legend, the reader is referred to the Web version of this article.)

during myogenesis.

3.7. SelK ablation leads to excessive ROS generation during myogenic differentiation

Throughout myogenic differentiation, increased ROS production serves as a signaling molecule to contribute to apoptosis and autophagy

and plays a vital role in initiating the activation of SCs [38,39]. Therefore, we tested whether SelK ablation changed the status of the redox environment during myogenic differentiation. As shown in Fig. 7A, we measured the activities of SOD, CAT and T-AOC as well as the levels of H_2O_2 and MDA in TA muscles at 5 d postinjury. We found that although activities of the two antioxidant enzymes (SOD and CAT) in wild-type mice were reversed during repair after skeletal muscle injury and the MDA content was not changed, H_2O_2 and T-AOC were increased. Silencing SelK significantly inhibited the activities of antioxidant enzymes and T-AOC and promoted H_2O_2 and MDA contents compared to controls, indicating that silencing SelK aggravates oxidative stress in vivo. Correspondingly, staining and quantification of intracellular ROS produced by C2C12 myoblasts using DCF-DA staining revealed a marked increase 1day after initiation of differentiation and reached a peak at day 3 (Fig. 7B and C). An abnormally high increase in ROS was observed in SelK knockdown cells compared to siNC cells, indicating again that SelK modulates the redox environment during myogenesis.

Subsequently, we explored the effect of appropriate alleviation of SelK-induced ROS overproduction on differentiation by treating cells with 1 mM NAC or 1 μM SF (two widely recognized antioxidants). As shown in Figs. S5A–D, exposing siNC or siSelK C2C12 myoblasts to NAC or SF at day 3 differentiation resulted in decreased ROS production, along with increased mRNA levels of SOD1, SOD2 and CAT, suggesting the success of these two antioxidants in attenuating oxidative stress. Moreover, consistent with previous research showing that excessive reductive stress impairs myogenic differentiation [40], we found that control cells exposed to NAC or SF treatment exhibited a reduced ratio of $MyHC^+$ and $MyoG^+$ cells and decreased expression of MRFs at the mRNA and protein levels after 5 days of differentiation (Fig. 7D-M and Figs. S5E and F), which were directly related to poor myotube formation. Intriguingly, when NAC or SF reduced SelK knockdown-aggravated ROS generation, the percentages of $MyHC^+$ and $MyoG^+$ cells were increased, and the inhibited differentiation of C2C12 myoblasts was efficiently rescued (Fig. 7D-M and Figs. S5E and F). In addition, the results of flow cytometry and quantitative analysis of apoptosis and autophagy-related marker genes showed that the additional treatment with NAC during

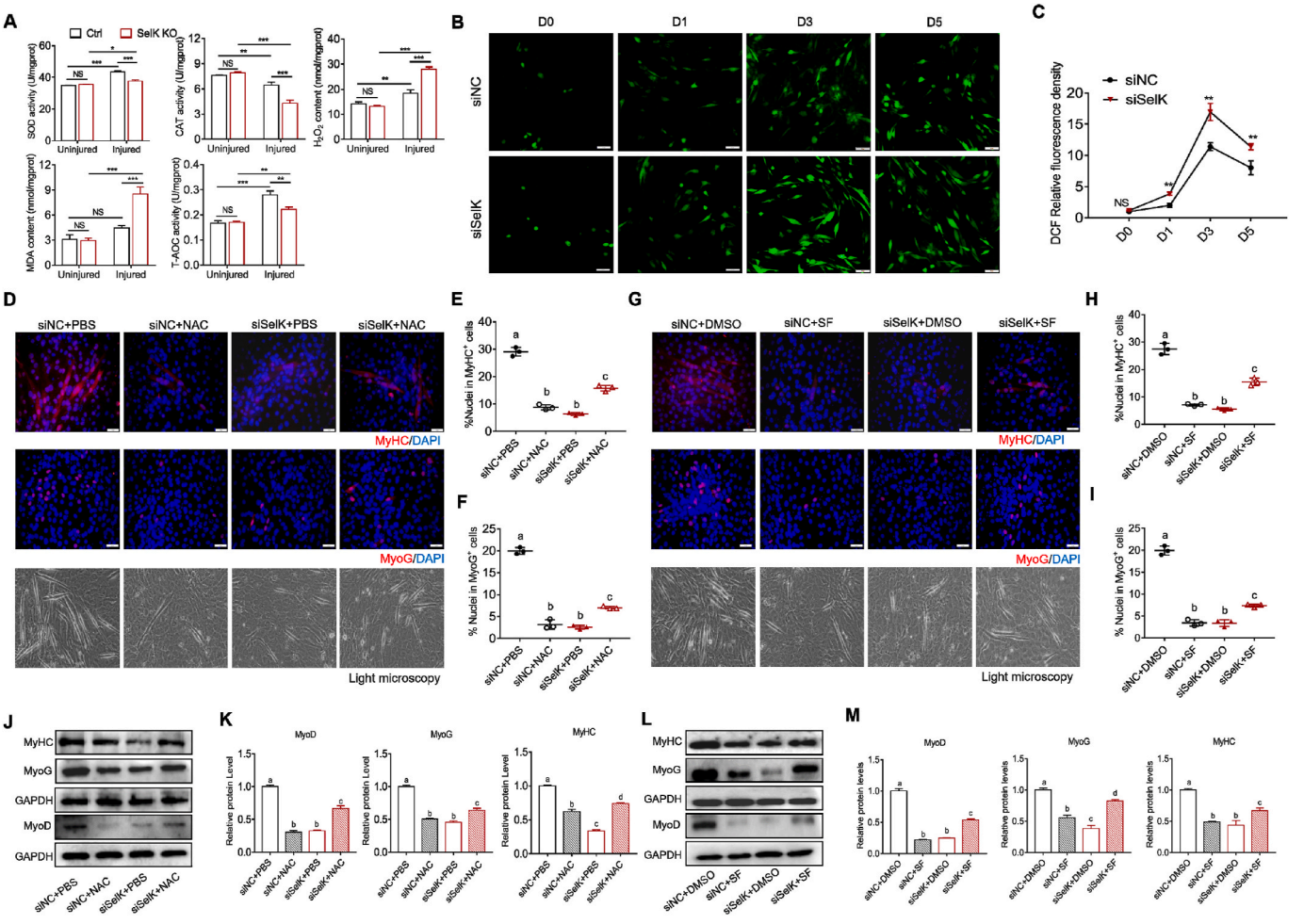

Fig. 7. Silencing of SelK enhances oxidative stress in SCs and C2C12 myoblast cells during myogenic differentiation. (A) Activities of antioxidant enzymes (SOD and CAT) and the contents of oxidative stress markers (H_2O_2, MDA and T-AOC) in TA muscles of Ctrl and SelK KO mice at 5 d postinjury (N = 3). **(B)** and **(C)** DCFH-DA staining and quantification of ROS generation in C2C12 myoblast cells cultured in differentiation medium for 0, 1, 3 and 5 d (N = 3). **(D)** Immunofluorescence staining of MyHC and MyoG and bright field microscopy in siNC and siSelK C2C12 myoblast cells treated with NAC or PBS after 5 d in differentiation medium (N = 3). **(E)** Quantitative analysis of the percentage of $MyHC^+$ cells and **(F)** the percentage of $MyoG^+$ cells treated with NAC or PBS after 5 d in differentiation medium. **(G)** Immunofluorescence staining of MyHC and MyoG and bright field microscopy in siNC and siSelK C2C12 myoblast cells treated with SF or DMSO after 5 d in differentiation medium (N = 3). **(H)** Quantitative analysis of the percentage of $MyHC^+$ cells and **(I)** the percentage of $MyoG^+$ cells treated with SF or DMSO after 5 d in differentiation medium. **(J)** and **(K)** Western blotting analysis of MyoD, MyoG and MyHC protein levels in siNC and siSelK C2C12 myoblast cells treated with NAC or PBS after 5 d in differentiation medium (N = 3). **(L)** and **(M)** Western blotting analysis of MyoD, MyoG and MyHC protein levels in siNC and siSelK C2C12 myoblast cells treated with SF or DMSO after 5 d in differentiation medium (N = 3). The results are presented as means ± S.D. *$p < 0.05$, **$p < 0.005$, ***$p < 0.001$, values significantly different from the corresponding control by unpaired *t*-test. Bars that do not share the same letters are significantly different ($p < 0.05$) from each other by one-way ANOVA.

differentiation reduced the percentage of Annexin V positive cells in both siNC group and siSelK groups, accompanied by decreased cleaved Cas3, Bax:Bcl2 ratio, LC3 II:LC3 I ratio and increased p62 (Fig, S6), suggesting that changes in the levels of apoptosis and autophagy caused by SelK silencing were closely related to ROS generation. Cumulatively, these data indicate that the regulation of ROS and oxidative stress may be a part of the mechanism of SelK in regulating myogenic differentiation.

3.8. SelK stabilizes ER stress-induced UPR of in myogenesis

In view of the role of SelK in regulating ERAD and the effect of ER stress on the myogenesis process, we tested the activation leveld of UPR-related proteins. As shown in Fig. 8A–C, $BaCl_2$ injected SelK KO mice showed significantly higher protein expression of ER chaperones and regulatory proteins (GRP78, ATF6, phospho-IRE1, phospho-PERK, phospho-eIF-2α and CHOP), accompanied by increased corresponding mRNA expression compared to wild-type mice. Meanwhile, in the process of inducing myogenic differentiation in vitro, we found that expression of these UPR marker genes in the siSelK C2C12 myoblasts increased correspondingly compared to that in the siNC cells (Figs. S7A and B). These data indicate that SelK ablation triggers excessive ER stress in myogenic cells during myogenesis. Next, to determine the relationship between ER stress and oxidative stress in response to SelK silencing, we treated cells with two classic ER stress inhibitors, 4-PBA (1 mM) or TUDCA (200 μM). Immunoblotting showed that 4-PBA or TUDCA effectively inhibited the SelK silencing-induced activation of UPR-related proteins and excessive oxidative stress (Fig. 8D–I and Figs. S7C and D). In contrast, exposing siSelK cells to antioxidant reagents (NAC or SF) to directly suppress increased ROS production did not change the expression of UPR-related proteins (Figs. S7E–H). Overall, these results strongly suggest that SelK regulates UPR homeostasis during myogenesis and that the generation of ROS caused by SelK ablation is mediated by aggravating ER stress.

Next, we investigated the performance of C2C12 myoblasts treated with ER stress inhibitors during differentiation. Immunofluorescence staining and light microscopy clearly showed that insufficient ER stress caused by 4-PBA or TUDCA significantly inhibited the process of myogenic differentiation in siNC cells and reduced the percentage of $MyoG^+$ and $MyHC^+$ cells and myotube formation (Fig. 8J-O). However, when we used 4-PBA or TUDCA to appropriately alleviate the ER stress caused by siSelK, the percentages of $MyHC^+$ and $MyoG^+$ cells were markedly increased, and the inhibited terminal differentiation of myoblasts into myotubes was rescued (Fig. 8J-O). qRT–PCR and

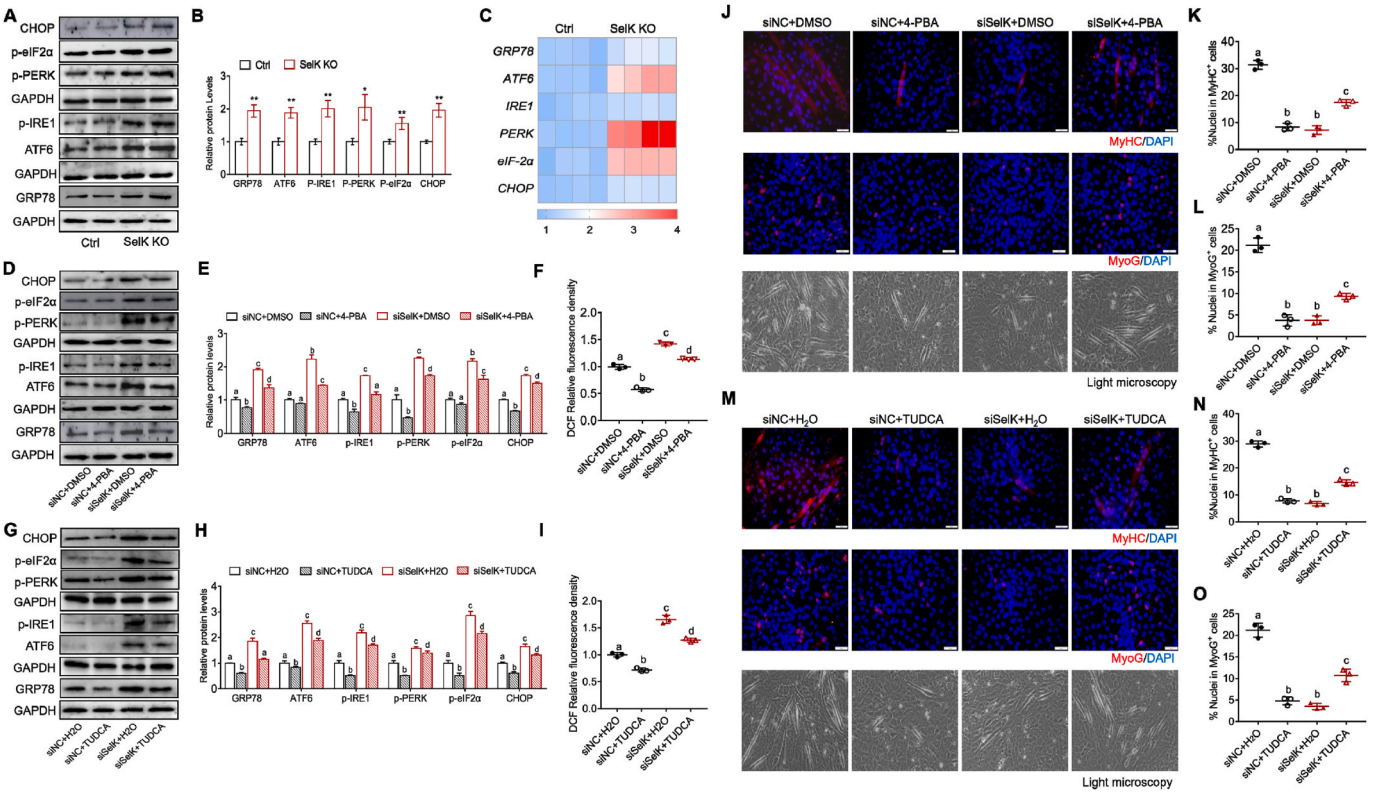

Fig. 8. Silencing SelK aggravates ER stress in SCs and C2C12 myoblast cells during myogenic differentiation. (A) and **(B)** Western blotting analysis of ER stress-related genes (GRP78, ATF6, p-IRE1, p-PERK, p-eIF-2α and CHOP) protein levels in the TA muscle of Ctrl and SelK KO mice at 5 d postinjury (N = 3). **(C)** qRT-PCR analysis of ER stress-related genes mRNA levels in the TA muscle of Ctrl and SelK KO mice at 5 d postinjuy (N = 3). **(D)** and **(E)** Western blotting analysis of ER stress-related genes protein levels in siNC and siSelK C2C12 myoblast cells treated with 4-PBA or DMSO after 5 d in differentiation medium (N = 3). **(F)** Quantification of DCFH-DA stained ROS generation in siNC and siSelK C2C12 myoblast cells treated with 4-PBA or DMSO after 3 d in differentiation medium. **(G)** and **(H)** Western blotting analysis of ER stress-related genes protein levels in siNC and siSelK C2C12 myoblast cells treated with TUDCA or H_2O after 5 d in differentiation medium (N = 3). **(I)** Quantification of DCFH-DA stained ROS generation in siNC and siSelK C2C12 myoblast cells treated with TUDCA or H_2O after 3 d in differentiation medium (N = 3). **(J)** Immunofluorescence staining of MyoG and MyHC and bright field microscopy in siNC and siSelK C2C12 myoblast cells treated with 4-PBA or DMSO after 5 d in differentiation medium (N = 3). **(K)** Quantitative analysis of the percentage of $MyHC^+$ cells and **(L)** the percentage of $MyoG^+$ cells treated with 4-PBA or DMSO after 5 d in differentiation medium. **(M)** Immunofluorescence staining of MyoG and MyHC and bright field microscopy in siNC and siSelK C2C12 cells treated with TUDCA or H_2O after 5 d in differentiation medium (N = 3). **(N)** Quantitative analysis of the percentage of $MyHC^+$ cells and **(O)** the percentage of MyoG $^+$ cells C2C12 cells treated with TUDCA or H_2O after 5 d in differentiation medium. The results are presented as means ± S.D. *$p < 0.05$, **$p < 0.005$, values significantly different from corresponding control by unpaired *t*-test. Bars that do not share the same letters are significantly different ($p < 0.05$) from each other by one-way ANOVA.

immunoblotting also demonstrated that expression of MRFs inhibited by siSelK silencing was relieved by 4-PBA or TUDCA (Fig. S7I-N). Meanwhile, flow cytometry and immunoblotting demonstrated that after adding 4-PBA to the siNC group, the levels of apoptosis and autophagy were inhibited, which was lower than the level required for the normal differentiation process. This effect allowed excessive autophagy and apoptosis in the siSelK group to be appropriately alleviated (Fig. S8). Collectively, intracellular ROS production is increased when SelK-mediated ER stress is upregulated, inducing excessive apoptosis and autophagy and diminishing myogenesis.

4. Discussion

Skeletal muscle injury and repair are closely related processes because the latter depends upon the timely activation and full differentiation of SCs in the background of destructive stress stimuli [41,42]. In the present investigation, we first demonstrated that SelK participates in regulating SCs fate and skeletal muscle regeneration. Data from the SelK KO mouse model confirmed that loss of SelK results in delayed myogenic differentiation. Genetic silencing of SelK exacerbated the ER stress-mediated UPR, ROS production, apoptosis and autophagy, which led to a negative influence on the myogenesis from an overall perspective (Fig. 9).

Increasing evidence has shown that some selenoproteins, such as selenoprotien O, selenoprotein P, and selenoprotein W function in maintaining intracellular homeostasis, playing crucial roles in various processes, such as chondrogenesis [43], adipogenesis, bone remodelling [44,45], and myogenesis [46]. SelK is a small transmembrane selenoprotein with a selenocysteine residue near the C-terminus [30]. Although a previous study showed that SelK levels were inhibited during preadipocytes differentiation into adipocytes [47], our results found that SelK was expressed in activated SCs and showed a gradual increasing trend with progression of myogenic differentiation, indicating a regulatory role for SelK in myogenesis. Supporting this finding, the rate of MyoG^{+} SCs in SelK KO mice was significantly decreased, and the potential of C2C12 myoblasts to differentiate into myotubes was reduced when expression of SelK was disrupted. Due to differences in gene expression between different developmental tissues, the opposite SelK level changes during the process of myogenesis and lipogenesis are acceptable and similar to the conclusion that the Islr gene is upregulated during SCs differentiation into myotubes but downregulated during mesenchymal stem cell differentiation into bone and adipose tissue [48]. In addition, accompanied by impaired myogenic differentiation in SelK KO mice and siSelK C2C12 myoblasts, excessive autophagy and apoptosis were identified in our study. Autophagy and apoptosis coexist in early muscle injury throughout regeneration because the former is responsible for cell reprogramming by regulating cytoplasmic remodelling, while the latter eliminates defective cells that do not have differentiation potential [49,50]. The crosstalk between apoptosis and autophagy determines the balance of cell survival and death, allowing SCs to differentiate normally [51]. However, improper autophagy and apoptosis hamper myotube formation and muscle regeneration [52,53]. Therefore, the role of SelK in myogenesis might involve the regulation of cell reprogramming and survival of SCs.

It is widely accepted that heightened ROS production-mediated redox regulation is associated with the myogenic program [13]. This increase in ROS in the controllable range is primarily dependent on changes in the activities of various enzymes in the antioxidant system. But when homeostasis of the antioxidant system is unbalanced and the level of oxidative stress exceeds the threshold, skeletal muscle

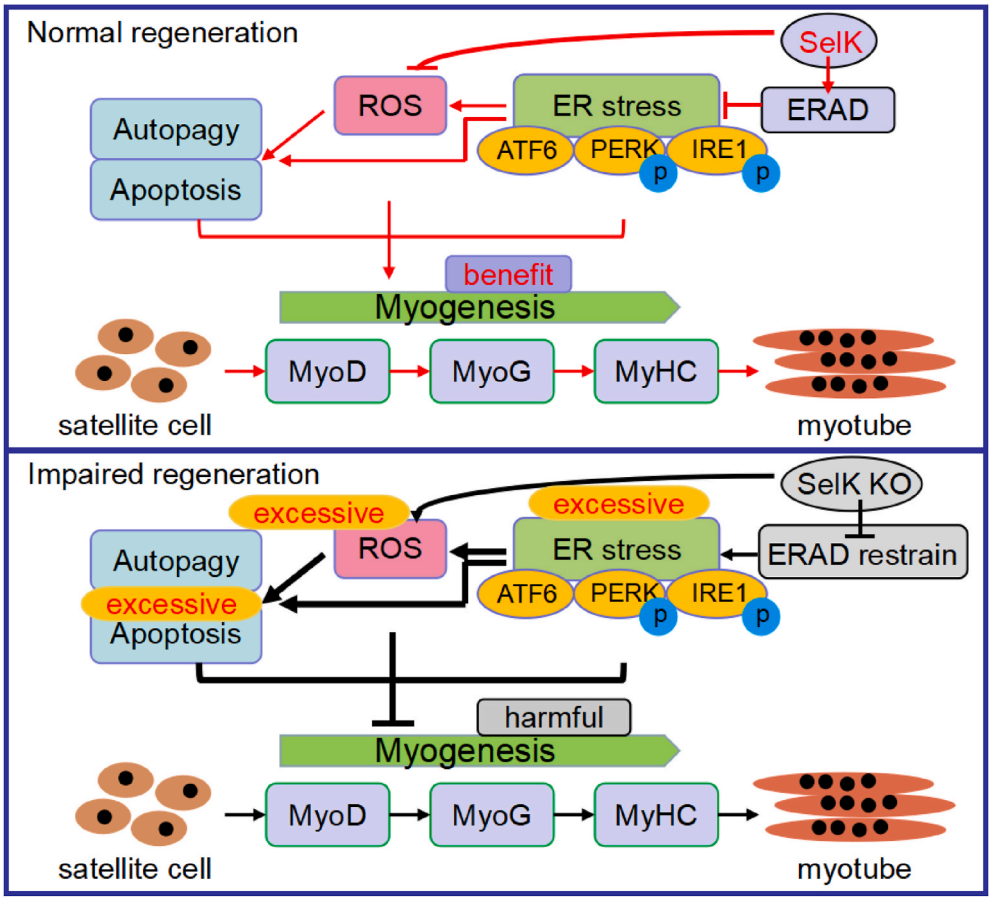

Fig. 9. Schematic diagram of the role of SelK during adult skeletal muscle regeneration. The pro-ERAD role of SelK prevents the excessive response of the ER stress-mediated UPR, resulting in moderate activation of ROS production, autophagy and apoptosis in skeletal muscle regeneration.

regeneration will be disrupted. In a cardiotoxin-induced TA muscle injury model, genetic ablation of Nrf2 impaired antioxidant gene expression and sustained the burden of ROS, displaying immature and smaller TA muscle fibers compared to their WT counterparts [54]. Meanwhile, extensive evidence has shown that excessive ROS initiates apoptosis and autophagy in multiple physiological or pathological conditions [55–57]. Similar to most selenoproteins, SelK has been reported to regulate the balance of cellular redox. In cardiomyocytes cultured in vitro, the transfected with SelK overexpression plasmid protects cells from H_2O_2-induced oxidative injury by reducing intracellular ROS level [31]. Silencing of SelK levels in N2a cells results in a decreased antioxidant ability in the cells and induces excessive apoptosis [58]. In the present study, we found that SelK silencing decreased the activities and expressions of antioxidant enzymes and induced excessive ROS generation during myogenesis, but after treating cells with NAC or SF, ROS levels were reduced, autophagy and apoptosis were alleviated, and myotube formation was promoted, indicating that SelK-regulated skeletal muscle regeneration involves the participation of oxidative signals. Notably, although our findings indicated that the absence of SelK promotes oxidative stress, in fact, due to its own protein conformational characteristics (selenocysteine is not in a recognizable redox motif), it has only weak peroxidase activity, which is not sufficient to cause significant changes in the redox environment in SCs [59]. Therefore, the significant antioxidant function of SelK during differentiation may be largely derived from its indirect effect of other biological functions.

The ER stress-mediated UPR regulates myogenesis by directly or indirectly controlling the expression of MRFs and the levels of apoptosis and autophagy [17]. It has been reported that inhibition of ER stress fails to maintain skeletal muscle strength and mass with resultant muscle wasting in naive mice or models of cancer cachexia [60]. However, improper activation of three signalling branches of the UPR (ATF6, IRE1 and PERK) cause diminished myofibers formation. For instance, forcibly triggering the phosphorylation of the PERK downstream molecule eIF2α or activation of CHOP leads to anti-myogenic modulation on the early differentiation event [61]. Overexpression of ATF6 and IRE1 contribute to muscle atrophy and weakness [62,63]. When misfolded proteins accumulate in the ER lumen, the load of protein folding is increased, which can activate UPR and be modulated by ERAD. It also has been reported that ER stress can promote ROS production [64]. As a component of ERAD complex, SelK plays an important role in regulating ER homeostasis because its promoter region contains a functional ERS response element gene sequence [30]. SelK can promote ERAD and reduce the accumulation of misfolded proteins and the intensity of UPR, thus being a negative regulator of the ER stress signaling [65]. Herein, it was reasonable to find that silencing of SelK exacerbated UPR marker genes expression in vivo and in vitro. Meanwhile, inhibition of ER stress in siSelK myoblasts under 4-PBA or TUDCA treatment partly relieved excessive ER stress and inhibited myotube formation, accompanied by a significant reduction in ROS. These results indicate that the promyogenesis function of SelK is likely to act through modulation of the UPR and ER stress during myogenic differentiation and that SelK regulates antioxidant signalling in an ER stress-dependent manner.

In summary, our findings highlights the roles played by SelK in the myogenic differentiation of SCs during muscle repair. Activation of the ER stress-initiated UPR is strictly regulated by SelK to limit ROS production, consequently preventing excessive autophagy-mediated degradation and apoptotic death. As current therapies aim to improve the regenerative capacity of SCs, our results potentially provide new avenues for the treatment of chronic and/or severe muscle injury.

Declaration of interest statement

The authors declare that they have no known competing financial interests or personal relationships that could have appeared to influence the work reported in this paper.

Acknowledgments

This study was supported by funding from the National Key Research and Development Program of China (No. 2016YFD0500501)

Appendix A. Supplementary data

Supplementary data to this article can be found online at https://doi.org/10.1016/j.redox.2022.102255.

References

[1] A.M.J. Sanchez, R.B. Candau, H. Bernardi, FoxO transcription factors: their roles in the maintenance of skeletal muscle homeostasis, Cell. Mol. Life Sci. 71 (9) (2014) 1657–1671.
[2] J.D.R. Knight, R. Kothary, The myogenic kinome: protein kinases critical to mammalian skeletal myogenesis, skelet. Muscle 1 (2011).
[3] Y. Wang, W. Xie, B. Liu, H. Huang, W. Luo, Y. Zhang, X. Pan, X.Y. Yu, Z. Shen, Y. Li, Stem cell-derived exosomes repair ischemic muscle injury by inhibiting the tumor suppressor Rb1-mediated NLRP3 inflammasome pathway, Signal Transduct. Target Ther. 6 (1) (2021) 121.
[4] S.B.P. Charge, M.A. Rudnicki, Cellular and molecular regulation of muscle regeneration, Physiol. Rev. 84 (1) (2004) 209–238.
[5] J.D. Bernet, J.D. Doles, J.K. Hall, K.K. Tanaka, T.A. Carter, B.B. Olwin, p38 MAPK signaling underlies a cell-autonomous loss of stem cell self-renewal in skeletal muscle of aged mice, Nat. Med. 20 (3) (2014) 265–271.
[6] J.G. Tidball, Regulation of muscle growth and regeneration by the immune system, Nat. Rev. Immunol. 17 (3) (2017) 165–178.
[7] P.S. Zammit, Function of the myogenic regulatory factors Myf5, MyoD, Myogenin and MRF4 in skeletal muscle, satellite cells and regenerative myogenesis, Semin. Cell Dev. Biol. 72 (2017) 19–32.
[8] J.V. Chakkalakal, K.M. Jones, M.A. Basson, A.S. Brack, The aged niche disrupts muscle stem cell quiescence, Nature 490 (7420) (2012) 355–360.
[9] F. Yue, P. Bi, C. Wang, T. Shan, Y. Nie, T.L. Ratliff, T.P. Gavin, S. Kuang, Pten is necessary for the quiescence and maintenance of adult muscle stem cells, Nat. Commun. 8 (2017) 14328.
[10] E. Le Moal, V. Pialoux, G. Juban, C. Groussard, H. Zouhal, B. Chazaud, R. Mounier, Redox control of skeletal muscle regeneration, Antioxidants Redox Signal. 27 (5) (2017) 276–310.
[11] R. Lesmana, R.A. Sinha, B.K. Singh, J. Zhou, K. Ohba, Y. Wu, W.W. Yau, B.H. Bay, P.M. Yen, Thyroid hormone stimulation of autophagy is essential for mitochondrial biogenesis and activity in skeletal muscle, Endocrinology 157 (1) (2016) 23–38.
[12] Y. Guan, N. Gao, H. Niu, Y. Dang, J. Guan, Oxygen-release microspheres capable of releasing oxygen in response to environmental oxygen level to improve stem cell survival and tissue regeneration in ischemic hindlimbs, J. Contr. Release 331 (2021) 376–389.
[13] E. Barbieri, P. Sestili, Reactive oxygen species in skeletal muscle signaling, J. Signal Transduct. 2012 (2012) 982794.
[14] J. Zhou, A. Li, X. Li, J. Yi, Dysregulated mitochondrial Ca(2+) and ROS signaling in skeletal muscle of ALS mouse model, Arch. Biochem. Biophys. 663 (2019) 249–258.
[15] G. Bjorklund, M. Dadar, J. Aaseth, S. Chirumbolo, J.J. Pen, Cancer-associated cachexia, reactive oxygen species and nutrition therapy, Curr. Med. Chem. 26 (31) (2019) 5728–5744.
[16] T.H. Youm, S.H. Woo, E.S. Kwon, S.S. Park, NADPH oxidase 4 contributes to myoblast fusion and skeletal muscle regeneration, Oxid. Med. Cell. Longev. 2019 (2019) 3585390.
[17] D. Afroze, A. Kumar, ER stress in skeletal muscle remodeling and myopathies, FEBS J. 286 (2) (2019) 379–398.
[18] C. Hetz, E. Chevet, S.A. Oakes, Proteostasis control by the unfolded protein response (vol 17, pg 829, 2015), Nat. Cell Biol. 17 (8) (2015) 1088, 1088.
[19] C. Hetz, The unfolded protein response: controlling cell fate decisions under ER stress and beyond, Nat. Rev. Mol. Cell Biol. 13 (2) (2012) 89–102.
[20] C. Hetz, S. Saxena, ER stress and the unfolded protein response in neurodegeneration, Nat. Rev. Neurol. 13 (8) (2017) 477–491.
[21] J. Hwang, L. Qi, Quality control in the endoplasmic reticulum: crosstalk between ERAD and UPR pathways, Trends Biochem. Sci. 43 (8) (2018) 593–605.
[22] K. Nakanishi, T. Sudo, N. Morishima, Endoplasmic reticulum stress signaling transmitted by ATF6 mediates apoptosis during muscle development, J. Cell Biol. 169 (4) (2005) 555–560.
[23] J. Alter, E. Bengal, Stress-induced C/EBP homology protein (CHOP) represses MyoD transcription to delay myoblast differentiation, PLoS One 6 (12) (2011), e29498.
[24] Y. Tokutake, K. Yamada, S. Hayashi, W. Arai, T. Watanabe, S. Yonekura, IRE1-XBP1 pathway of the unfolded protein response is required during early differentiation of C2C12 myoblasts, Int. J. Mol. Sci. 21 (1) (2019).
[25] S. Li, F. Gao, J. Huang, Y. Wu, S. Wu, X.G. Lei, Regulation and function of avian selenogenome, Biochim. Biophys. Acta Gen. Subj. 1862 (11) (2018) 2473–2479.
[26] P. Chariot, O. Bignani, Skeletal muscle disorders associated with selenium deficiency in humans, Muscle Nerve 27 (6) (2003) 662–668.
[27] G.J. Fredericks, P.R. Hoffmann, Selenoprotein K and protein palmitoylation, Antioxidants Redox Signal. 23 (10) (2015) 854–862.

[28] S. Verma, F.W. Hoffmann, M. Kumar, Z. Huang, K. Roe, E. Nguyen-Wu, A. S. Hashimoto, P.R. Hoffmann, Selenoprotein K knockout mice exhibit deficient calcium flux in immune cells and impaired immune responses, J. Immunol. 186 (4) (2011) 2127–2137.
[29] H.D. Yao, Q. Wu, Z.W. Zhang, J.L. Zhang, S. Li, J.Q. Huang, F.Z. Ren, S.W. Xu, X. L. Wang, X.G. Lei, Gene expression of endoplasmic reticulum resident selenoproteins correlates with apoptosis in various muscles of se-deficient chicks, J. Nutr. 143 (5) (2013) 613–619.
[30] V.A. Shchedrina, R.A. Everley, Y. Zhang, S.P. Gygi, D.L. Hatfield, V.N. Gladyshev, Selenoprotein K binds multiprotein complexes and is involved in the regulation of endoplasmic reticulum homeostasis, J. Biol. Chem. 286 (50) (2011) 42937–42948.
[31] C. Lu, F. Qiu, H. Zhou, Y. Peng, W. Hao, J. Xu, J. Yuan, S. Wang, B. Qiang, C. Xu, X. Peng, Identification and characterization of selenoprotein K: an antioxidant in cardiomyocytes, FEBS Lett. 580 (22) (2006) 5189–5197.
[32] W. Shengchen, L. Jing, Y. Yujie, W. Yue, X. Shiwen, Polystyrene microplastics-induced ROS overproduction disrupts the skeletal muscle regeneration by converting myoblasts into adipocytes, J. Hazard Mater. 417 (2021) 125962.
[33] Q. Chi, Q. Zhang, Y. Lu, Y. Zhang, S. Xu, S. Li, Roles of selenoprotein S in reactive oxygen species-dependent neutrophil extracellular trap formation induced by selenium-deficient arteritis, Redox Biol. 44 (2021) 102003.
[34] T. Yang, C. Cao, J. Yang, T. Liu, X.G. Lei, Z. Zhang, S. Xu, miR-200a-5p regulates myocardial necroptosis induced by Se deficiency via targeting RNF11, Redox Biol. 15 (2018) 159–169.
[35] Z. Liu, X. Zhang, H. Lei, N. Lam, S. Carter, O. Yockey, M. Xu, A. Mendoza, E. R. Hernandez, J.S. Wei, J. Khan, M.E. Yohe, J.F. Shern, C.J. Thiele, CASZ1 induces skeletal muscle and rhabdomyosarcoma differentiation through a feed-forward loop with MYOD and MYOG, Nat. Commun. 11 (1) (2020) 911.
[36] M. Buckingham, P.W. Rigby, Gene regulatory networks and transcriptional mechanisms that control myogenesis, Dev. Cell 28 (3) (2014) 225–238.
[37] B.L. Baechler, D. Bloemberg, J. Quadrilatero, Mitophagy regulates mitochondrial network signaling, oxidative stress, and apoptosis during myoblast differentiation, Autophagy 15 (9) (2019) 1606–1619.
[38] S. Lee, E. Tak, J. Lee, M.A. Rashid, M.P. Murphy, J. Ha, S.S. Kim, Mitochondrial H2O2 generated from electron transport chain complex I stimulates muscle differentiation, Cell Res. 21 (5) (2011) 817–834.
[39] J.H. Kim, T.G. Choi, S. Park, H.R. Yun, N.N.Y. Nguyen, Y.H. Jo, M. Jang, J. Kim, J. Kim, I. Kang, J. Ha, M.P. Murphy, D.G. Tang, S.S. Kim, Mitochondrial ROS-derived PTEN oxidation activates PI3K pathway for mTOR-induced myogenic autophagy, Cell Death Differ. 25 (11) (2018) 1921–1937.
[40] N.S. Rajasekaran, S.B. Shelar, D.P. Jones, J.R. Hoidal, Reductive stress impairs myogenic differentiation, Redox Biol. 34 (2020) 101492.
[41] J.G. Tidball, Mechanisms of muscle injury, repair, and regeneration, Compr. Physiol. 1 (4) (2011) 2029–2062.
[42] T. Endo, Molecular mechanisms of skeletal muscle development, regeneration, and osteogenic conversion, Bone 80 (2015) 2–13.
[43] J. Yan, Y. Fei, Y. Han, S. Lu, Selenoprotein O deficiencies suppress chondrogenic differentiation of ATDC5 cells, Cell Biol. Int. 40 (10) (2016) 1033–1040.
[44] I. Dreher, N. Schutze, A. Baur, K. Hesse, D. Schneider, J. Kohrle, F. Jakob, Selenoproteins are expressed in fetal human osteoblast-like cells, Biochem. Biophys. Res. Commun. 245 (1) (1998) 101–107.
[45] Y. Zhang, X. Chen, Reducing selenoprotein P expression suppresses adipocyte differentiation as a result of increased preadipocyte inflammation, Am. J. Physiol. Endocrinol. Metab. 300 (1) (2011) E77–E85.
[46] Y.H. Jeon, Y.H. Park, J.H. Lee, J.H. Hong, I.Y. Kim, Selenoprotein W enhances skeletal muscle differentiation by inhibiting TAZ binding to 14-3-3 protein, Biochim. Biophys. Acta 1843 (7) (2014) 1356–1364.
[47] J.H. Lee, J.K. Jang, K.Y. Ko, Y. Jin, M. Ham, H. Kang, I.Y. Kim, Degradation of selenoprotein S and selenoprotein K through PPARgamma-mediated ubiquitination is required for adipocyte differentiation, Cell Death Differ. 26 (6) (2019) 1007–1023.
[48] K. Zhang, Y. Zhang, L. Gu, M. Lan, C. Liu, M. Wang, Y. Su, M. Ge, T. Wang, Y. Yu, C. Liu, L. Li, Q. Li, Y. Zhao, Z. Yu, F. Wang, N. Li, Q. Meng, Islr regulates canonical Wnt signaling-mediated skeletal muscle regeneration by stabilizing Dishevelled-2 and preventing autophagy, Nat. Commun. 9 (1) (2018) 5129.
[49] A. Saera-Vila, P.E. Kish, K.W. Louie, S.J. Grzegorski, D.J. Klionsky, A. Kahana, Autophagy regulates cytoplasmic remodeling during cell reprogramming in a zebrafish model of muscle regeneration, Autophagy 12 (10) (2016) 1864–1875.
[50] Y. Nie, S. Cai, R. Yuan, S. Ding, X. Zhang, L. Chen, Y. Chen, D. Mo, Zfp422 promotes skeletal muscle differentiation by regulating EphA7 to induce appropriate myoblast apoptosis, Cell Death Differ. 27 (5) (2020) 1644–1659.
[51] A. Jiang, H. Guo, W. Wu, H. Liu, The crosstalk between autophagy and apoptosis is necessary for myogenic differentiation, J. Agric. Food Chem. 69 (13) (2021) 3942–3951.
[52] S.A. Fernandes, C.F. Almeida, L.S. Souza, M. Lazar, P. Onofre-Oliveira, G. L. Yamamoto, L. Nogueira, L.Y. Tasaki, R.R. Cardoso, R.C.M. Pavanello, H.C. A. Silva, M.F.R. Ferrari, A. Bigot, V. Mouly, M. Vainzof, Altered in vitro muscle differentiation in X-linked myopathy with excessive autophagy, Dis. Model. Mech. 13 (2) (2020).
[53] G. Xiong, S.M. Hindi, A.K. Mann, Y.S. Gallot, K.R. Bohnert, D.R. Cavener, S. R. Whittemore, A. Kumar, The PERK arm of the unfolded protein response regulates satellite cell-mediated skeletal muscle regeneration, Elife 6 (2017).
[54] S.B. Shelar, M. Narasimhan, G. Shanmugam, S.H. Litovsky, S.S. Gounder, G. Karan, C. Arulvasu, T.W. Kensler, J.R. Hoidal, V.M. Darley-Usmar, N.S. Rajasekaran, Disruption of nuclear factor (erythroid-derived-2)-like 2 antioxidant signaling: a mechanism for impaired activation of stem cells and delayed regeneration of skeletal muscle, Faseb. J. 30 (5) (2016) 1865–1879.
[55] L.J. Su, J.H. Zhang, H. Gomez, R. Murugan, X. Hong, D. Xu, F. Jiang, Z.Y. Peng, Reactive oxygen species-induced lipid peroxidation in apoptosis, autophagy, and ferroptosis, Oxid. Med. Cell. Longev. (2019) 5080843, 2019.
[56] L. Wang, L. Wang, X. Shi, S. Xu, Chlorpyrifos induces the apoptosis and necroptosis of L8824 cells through the ROS/PTEN/PI3K/AKT axis, J. Hazard Mater. 398 (2020) 122905.
[57] Z. Miao, Z. Miao, S. Wang, H. Wu, S. Xu, Exposure to imidacloprid induce oxidative stress, mitochondrial dysfunction, inflammation, apoptosis and mitophagy via NF-kappaB/JNK pathway in grass carp hepatocytes, Fish Shellfish Immunol. 120 (2022) 674–685.
[58] S.Z. Jia, X.W. Xu, Z.H. Zhang, C. Chen, Y.B. Chen, S.L. Huang, Q. Liu, P. R. Hoffmann, G.L. Song, Selenoprotein K deficiency-induced apoptosis: a role for calpain and the ERS pathway, Redox Biol. 47 (2021) 102154.
[59] J. Liu, Z. Zhang, S. Rozovsky, Selenoprotein K form an intermolecular diselenide bond with unusually high redox potential, FEBS Lett. 588 (18) (2014) 3311–3321.
[60] K.R. Bohnert, Y.S. Gallot, S. Sato, G. Xiong, S.M. Hindi, A. Kumar, Inhibition of ER stress and unfolding protein response pathways causes skeletal muscle wasting during cancer cachexia, Faseb. J. 30 (9) (2016) 3053–3068.
[61] J.R. Jheng, Y.S. Chen, U.I. Ao, D.C. Chan, J.W. Huang, K.Y. Hung, D.C. Tarng, C. K. Chiang, The double-edged sword of endoplasmic reticulum stress in uremic sarcopenia through myogenesis perturbation, J. Cachexia Sarcopenia Muscle 9 (3) (2018) 570–584.
[62] D. Chen, Y. Wang, E.R. Chin, Activation of the endoplasmic reticulum stress response in skeletal muscle of G93A*SOD1 amyotrophic lateral sclerosis mice, Front. Cell. Neurosci. 9 (2015) 170.
[63] E.M. Clark, H.J.T. Nonarath, J.R. Bostrom, B.A. Link, Establishment and validation of an endoplasmic reticulum stress reporter to monitor zebrafish ATF6 activity in development and disease, Dis. Model. Mech. 13 (1) (2020).
[64] S. Chakravarthi, C.E. Jessop, N.J. Bulleid, The role of glutathione in disulphide bond formation and endoplasmic-reticulum-generated oxidative stress, EMBO Rep. 7 (3) (2006) 271–275.
[65] J.H. Lee, K.J. Park, J.K. Jang, Y.H. Jeon, K.Y. Ko, J.H. Kwon, S.R. Lee, I.Y. Kim, Selenoprotein S-dependent selenoprotein K binding to p97(VCP) protein is essential for endoplasmic reticulum-associated degradation, J. Biol. Chem. 290 (50) (2015) 29941–29952.